A Highly Conserved Arginine Is Critical for the Functional Folding of Inhibitor of Apoptosis (IAP) BIR Domains

3 AUTHORS, INCLUDING:

Laura Elena Luque de Johnson
Rhodes College
9 PUBLICATIONS   130 CITATIONS

A Highly Conserved Arginine Is Critical for the Functional Folding of Inhibitor of Apoptosis (IAP) BIR Domains

Laura E. Luque, Katrina P. Grape, and Matthew Junker*

Department of Molecular and Cell Biology, University of Texas at Dallas, P.O. Box 830688, Richardson, Texas 75083-0688

Received July 2, 2002; Revised Manuscript Received September 17, 2002

ABSTRACT: The inhibitor of apoptosis (IAP) proteins are found in all animals and regulate apoptosis (programmed cell death) by binding and inhibiting caspase proteases. This inhibition is overcome by several apoptosis stimulators, including *Drosophila* Hid and mammalian Smac/DIABLO, which bind to 65-residue baculovirus IAP repeat (BIR) domains found in one to three copies in all IAPs. Virtually all BIRs contain three Cys and a His that bind zinc, a Gly in a tight turn, and an Arg. The functional and structural role of the Arg was investigated in isolated BIR domains from the baculovirus *Orgyia pseudotsugata* Op-IAP and the *Drosophila* DIAP1 proteins. Mutation of the Arg to either Ala or Lys abolished Hid and Smac binding to BIRs, despite the Hid/Smac binding site being located on the opposite side of the BIR domain from the Arg. The mutant BIR domains also exhibited weakened zinc binding, increased sensitivity to limited proteolysis, and altered circular dichroism spectra indicative of perturbed domain folding. Examination of known BIR structures indicates that the Arg side chain makes simultaneous bridging hydrogen bonds and a cation−π interaction for which the Arg guanidino group is uniquely well suited. These interactions are likely critical for stabilizing the tertiary fold of BIR domains in all IAPs, explaining the conservation of this residue.

Apoptosis is programmed cell death, a process conserved in all animals which eliminates superfluous or potentially harmful cells. Apoptosis is required for normal embryogenesis and development and provides protection when triggered in cells infected by viruses or stressed by events such as severe DNA damage. At the core of the apoptotic process are caspase proteases whose activation in a proteolytic cascade commits a cell to destruction. Multiple distinct pathways converge to control the initiation of the caspase cascade, including those triggered by extracellular stimuli and others originating within the cell. Dysfunction in the regulation of apoptosis is associated with neurodegenerative diseases and cancer (*1−3*).

Members of the IAP[1] (inhibitor of apoptosis) family of proteins are found in all animals and regulate apoptosis in large part by binding and inhibiting the caspase proteases required for apoptosis (*4, 5*). This inhibition is overcome by several apoptosis stimulators which bind to IAPs, including Reaper, Grim, and Hid in *Drosophila* and Smac (or DI-ABLO) in mammals. Stimulation likely depends on the relative concentrations of stimulators and inhibitors, as high concentrations of IAPs can protect cells from expression of apoptosis stimulators (e.g., refs *6−9*). Members of the IAP family include human XIAP, NAIP, and survivin, *Drosophila* DIAP1, and baculovirus *Orgyia pseudotsugata* Op-IAP.

Genes for IAPs have been identified in insects, birds, fish, mammals, and viruses.

IAPs contain one, two, or three repeats of a conserved 65-residue sequence called the BIR (baculovirus inhibitor of apoptosis repeat) motif which is required for stimulator binding and for stimulator regulation of IAP-caspase inhibition. Three-dimensional structures have been determined for the single BIR-containing survivin as well as for individual BIRs of cIAP1, XIAP, and DIAP1 (*10−19*). As expected from sequence homology, all structures are very similar for the core 65-residue BIR motif which is comprised of four α helices with an intervening three-strand β sheet and a single bound zinc ion. Structures of BIR domain−stimulator complexes show the N-termini of Smac, Grim, Hid, and the recently identified *Drosophila* Sickle to bind to a surface groove between the final β strand and following helix in the BIR domain (*16, 17, 19, 20*). How BIR−stimulator association leads to activation of IAP-bound caspases varies. For the BIR3 of XIAP, the BIR surface groove also binds caspase-9, so that Smac−BIR3 association competitively dissociates and activates caspase-9 (*21*). For the BIR2 of XIAP, Smac association activates caspase-3 and caspase-7 molecules bound to residues adjacent to the BIR domain (*18, 22, 23*). However, in both of these cases a BIR domain is integral to the stimulator activation of IAP-bound caspases.

The Pfam database of protein domains lists 128 BIR sequences from 69 distinct BIR-containing proteins (non-fragmented BIR sequences in entry PF00653, version 7.3) (*24*). These proteins derive from yeast, nematodes, insects, birds, mammals, and 19 different viruses. When aligned, they generate a consensus BIR sequence at an 85% threshold level of R-X$_2$-OF-X$_{2−4}$-a-X$_{5−10}$-pXh-X$_3$-Ghha-X$_{2−6}$-pX$_{2−6}$-ChXC-

---

* To whom correspondence should be addressed. Phone: (972) 883-2514. Fax: (972) 883-2409. E-mail: mjunker@utdallas.edu.

[1] Abbreviations: BIR, baculovirus inhibitor of apoptosis repeat; BME, β-mercaptoethanol; CD, circular dichroism; IAP, inhibitor of apoptosis; EDTA, ethylenediaminetetraacetic acid; IPTG, isopropyl β-D-thiogalactopyranoside; MBP, maltose binding protein; PCR, polymerase chain reaction; PMSF, phenylmethanesulfonyl fluoride; SDS−PAGE, sodium dodecyl sulfate−polyacrylamide gel electrophoresis.

X$_3$-h-X$_2$-aX$_3$-pphhXp<u>H</u>-X$_5$-p<u>C</u>Xah, where X is any residue, O is Ser or Thr, and a, p, and h are aromatic, polar, and hydrophobic residues, respectively. The six residues underlined in this consensus sequence are almost invariant, being absent in no more than two BIR sequences, which suggests that they are critical for BIR domain structure and/or function. In the three-dimensional structures of BIR domains, the His and three Cys residues coordinate a single zinc ion in a Cys$_2$HisCys zinc fingerlike site underlying the surface groove where the N-termini of Smac, Grim, and Hid bind. The conserved Gly also appears to play a critical structural role as it is in a sharp turn and adopts backbone torsion angles that are unfavorable for all other amino acids ($\phi \sim 85°$, $\psi \sim 0°$). The role of the highly conserved Arg in BIR domains is less clear. It is located near the N-terminus of the first BIR α helix, on the side of the BIR domain opposite to that of the apoptosis stimulator binding groove, and with its side chain mostly buried. The Arg is absent in only one of the 128 BIR sequences and shifted one residue in another. By comparison, one of the zinc-binding Cys is absent in two sequences and another is absent in one.

Mutation of the highly conserved Arg to Ala in the second BIR (BIR2) domain of the baculovirus *O. pseudotsugata* Op-IAP abolished Op-IAP inhibition of Hid in insect cells, indicating that this Arg is critical for BIR function (*8*). To determine the role of the conserved Arg, we analyzed the structural and functional consequences of mutating this Arg in isolated BIR domains in vitro. The analysis finds that the guanidino group of the Arg is required for the structural stability of the BIR domain, and mutation of the Arg causes structural alterations that propagate through the zinc site to the apoptosis stimulator-binding groove on the opposite face of the BIR domain. The structural stabilization is likely the result of hydrogen bonding and a cation−π interaction made by the Arg with conserved aromatic residues. Since these interactions involve residues spaced far in sequence, they are likely critical in directing and stabilizing the tertiary fold of BIR domains.

MATERIALS AND METHODS

Protein Expression Plasmids. Plasmids for recombinant expression of BIR domains fused to the maltose binding protein (MBP) were generated by inserting BIR-encoding DNA into the pMAL-c2 expression plasmid (New England BioLabs). Full-length copies of the genes for Op-IAP, DIAP1, and the Op-IAP Arg114Ala mutant were obtained from the laboratory of Dr. Lois K. Miller (University of Georgia) in the plasmids pHSEpiOpIAPVI+, pHSEpiOpIAPVI+ R114A, and pHSP70PLVI+ Epi Diap1, respectively. DNA duplexes encoding the wild-type and Arg114Ala mutant BIR2 regions of Op-IAP (residues 95−199) and of wild-type DIAP1 (residues 210−314) were amplified from these plasmids by PCR. Primer pairs for the Op-IAP BIR2 regions were CGCGCTCCGCCGGCTCGGTCGGCTGCCGCGC and GTGCGCTTCGGGATCCTAGTCGCGAACCACACACG. Primer pairs for the DIAP1 BIR2 region were TCAGCCGCCAGTGGCAATTATTTTCC and GAAGTGCTCGGATCCTACTCCTCGGC. Following restriction digestion with *Bam*HI, the amplified BIR sequences were inserted into the *Xmn*I and *Bam*HI sites in pMAL-c2 to create the plasmids pMAL-Op-IAP-BIR2, pMAL-Op-IAP-BIR2 (Arg114Ala), and pMAL-DIAP1-BIR2.

MBP-BIR fusions for the Arg114Lys mutant of Op-IAP and the Arg229Lys mutant of DIAP1 were generated by site-directed mutagenesis using the "megaprimer" method (*25*). For the Op-IAP Arg mutation, a megaprimer was generated from the pMAL-Op-IAP-BIR2 plasmid by PCR using a primer pair of CACGGAAGCCGCGAAATTGCGCACCTTTG (introducing the Lys mutation at codon 114) and CCATCGCAGCAAAAGCACCGCGTCTTG (allowing amplification to the *Psh*AI site centered at codon 153). A second round of PCR with the pMAL-Op-IAP−BIR2 template was then performed with the megaprimer and an upstream primer that overlapped the *Nco*I site in the MalE gene of the pMAL host vector (primer sequence TATTGCCACCATGGAAAACGCCCAGAAAGG). Following restriction digestion with *Nco*I and *Psh*AI, the amplified PCR product was inserted into the *Nco*I and *Psh*AI sites of pMAL-Op-IAP-BIR2 to create pMAL-Op-IAP-BIR2 Arg114Lys. For the DIAP1 Arg mutation, a megaprimer was first generated from the pMAL-DIAP1-BIR2 plasmid by PCR using the primers CGAGACGGCAAAACTGCGTACCTTCGAGG (introducing the Lys mutation to codon 229) and GGCCACCGTATCGATATAGAGCTGA (allowing amplification to the *Cla*I site at codon 302). A second round of PCR then used this megaprimer and the same upstream primer with the *Nco*I site as used for the Op-IAP Arg mutation. Insertion of this PCR product into the *Nco*I and *Cla*I sites of pMAL-DIAP1-BIR2 produced the pMAL-DIAP1-BIR2 (Arg229Lys) plasmid. The sequences of all constructed plasmids were verified by DNA sequencing.

The Hid(1−37)-GST-His$_6$ fusion protein was expressed from a pET23a (+)-derived plasmid obtained from the laboratory of Dr. Bruce Hay (California Institute of Technology). Smac fused to a C-terminal His$_6$ tag was expressed from a plasmid obtained from the laboratory of Dr. Xiaodong Wang (University of Texas Southwestern Medical Center).

Protein Expression and Purification. MBP-BIR fusions were expressed in *Escherichia coli* BL21 cells grown in LB media at 37 °C. Protein expression was induced by addition of 50 μM IPTG and 50 μM Zn$_2$SO$_4$. Following 3−4 h postinduction growth, cells were pelleted, resuspended in 20 mM Tris, 200 mM KCl, 1 mM PMSF, and 5 mM BME, pH 8, and lysed by sonication. Lysates were centrifuged at 27000g, and the supernatants were applied to a Q-Sepharose (Amersham Pharmacia Biotech) column equilibrated with 20 mM Tris, 25 mM NaCl, 10 μM ZnCl$_2$, and 5 mM BME at pH 8. MBP-BIR fusions typically eluted between 150 and 300 mM NaCl, although some BIR mutants did not bind to the Q-Sepharose and were collected in the flow-through. Pooled MBP-BIR fractions were then applied to an amylose (New England BioLabs) column equilibrated with 20 mM Tris, 150 mM NaCl, 10 μM ZnCl$_2$, and 5 mM BME at pH 8 from which MBP-BIR fusions were eluted with 10 mM maltose. Removal of maltose for subsequent use of MBP-BIRs in the stimulator-binding assays was achieved by washing the MBP-BIRs on a second Q-Sepharose column followed by elution with a step gradient of 300 mM NaCl. For refolding reactions, MBP-BIR proteins were denatured in 7 M urea, 20 mM Tris, 150 mM NaCl, 0.1 mM EDTA, and 5 mM BME at a maximum protein concentration of 4 μM. Protein was then dialyzed against a series of buffers containing successively reduced urea concentrations (3 M,
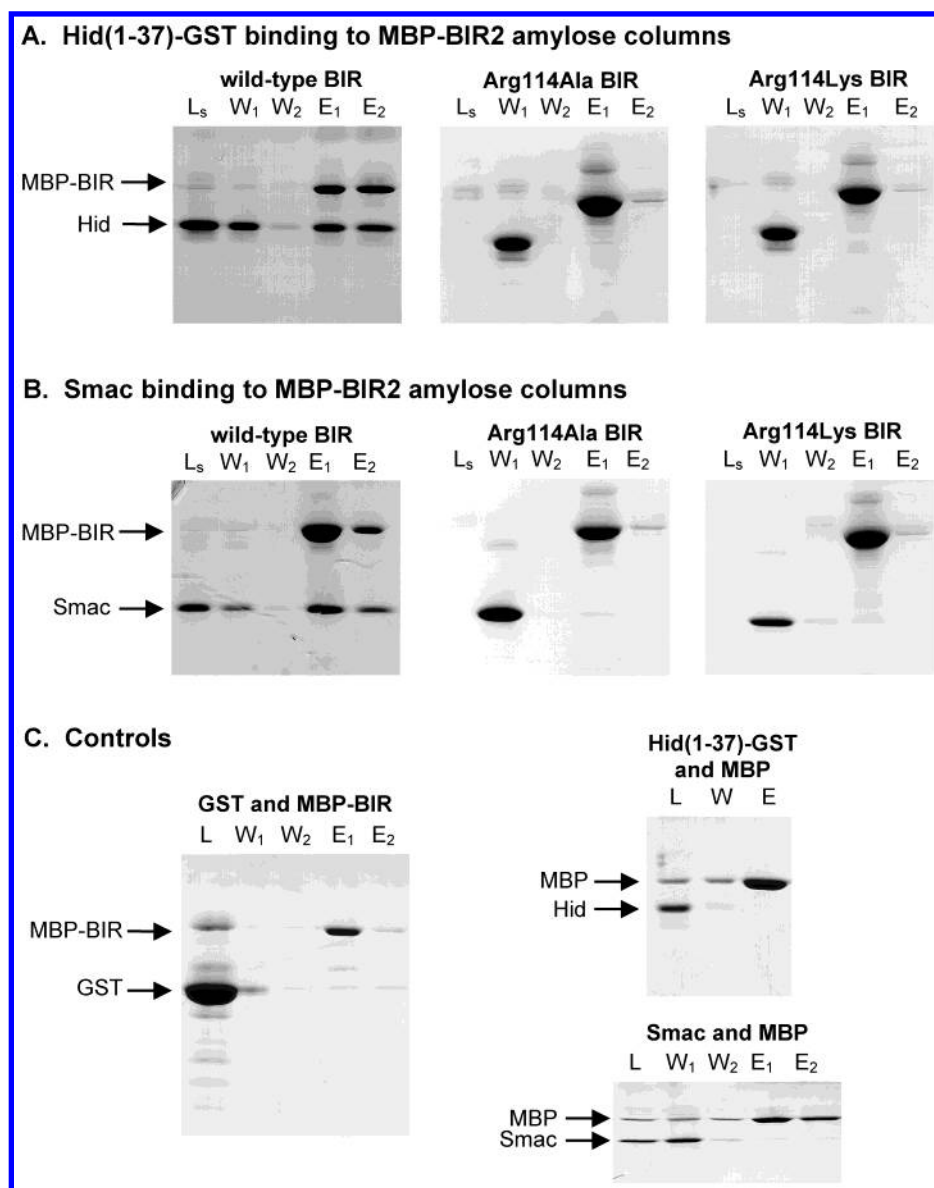
FIGURE 1: Coomassie-stained SDS−PAGE gels of Hid(1−37)-GST (A) and Smac (B) binding to wild-type and mutant MBP-Op-IAP-BIR2 fusions. The MBP-BIR fusions were immobilized on amylose columns and eluted with maltose. The gel lanes show column elutions during application of Hid or Smac (L$_s$; 4 nmol for wild-type BIR, 12 nmol for mutant BIRs), washes with 1 mL of buffer each (W$_1$, W$_2$), and elution with 10 mM maltose (E$_1$, E$_2$). Control experiments in panel C demonstrate no binding of GST alone (no Hid) to wild-type MBP-BIR-amylose, no binding of Hid(1−37)-GST to MBP-amylose (no BIR), and no binding of Smac to MBP-amylose (no BIR).

1 M, and twice against 0 M urea) containing 20 mM Tris, 150 mM NaCl, 10 μM ZnCl$_2$, and 5 mM BME at pH 8. Following dialysis, the refolded proteins were washed on a Q-Sepharose column to remove residual urea. Isolated BIR domains were prepared by cleaving BIR domains from MBP using factor X$_a$ protease (New England BioLabs) and separating the BIR domains from MBP by amylose and Mono Q (Pharmacia) chromatographies.

Recombinant Hid(1−37)-GST-His$_6$ and Smac-His$_6$ proteins were expressed in *E. coli* BL21-DE3 cells and partially purified by Q-Sepharose as with the MBP-BIR fusions. Further purification was achieved by nickel-NTA (Qiagen) chromatography in which Hid and Smac were eluted in 250 mM imidazole. Both Hid and Smac were then dialyzed into 20 mM Tris and 150 mM NaCl at pH 8. The Hid buffer also contained 5 mM BME.

Protein concentrations were determined by absorbance at 280 nm. Extinction coefficients of 94200, 96500, and 89500

M^{-1} cm^{-1} for MBP-Op-IAP-BIR2, MBP-Op-IAP-BIR2 (Arg114Lys), and MBP-DIAP1-BIR2, respectively, were determined by comparing the absorbance spectrum of each protein under native conditions with the spectrum when denatured in 6 M guanidine hydrochloride, where extinction coefficients were directly calculated. Since folded and denatured extinction coefficients differed by less than 10%, all other protein concentrations were determined using calculated extinction coefficients.

Binding Assays. Binding of Hid(1−37)-GST and Smac to MBP-BIRs was assayed using an affinity column-based assay. Small amylose columns (approximately 100 μL bed volume) equilibrated with binding buffer (20 mM Tris, 150 mM NaCl, 10 μM ZnCl$_2$, 5 mM BME, pH 8) were prebound with saturating amounts of MBP-BIR. The columns were then washed twice with 2 mL of binding buffer to remove any overloaded protein. The columns were then loaded with excess Hid-GST or Smac at concentrations of 4 μM followed

by two 1 mL washes with binding buffer. A final elution was performed with binding buffer containing 10 mM maltose applied in two 400 μL aliquots. Samples of column elutions at each step were analyzed by SDS−PAGE stained with Coomassie dye.

Other Methods. Zinc quantitation was performed by flame atomic absorption on a Varian SpectrAA-5 spectrophotometer. Circular dichroism was performed on a Jasco J-710 spectropolarimeter with samples prepared in 15 mM potassium phosphate, 10 mM KCl, and 2 μM ZnCl$_2$ at pH 6.5. Proteolytic digests with thermolysin (Sigma) were performed at 4 °C with 1 μg/mL thermolysin and 10 μM MBP-BIR substrate in 20 mM Tris, 300 mM NaCl, 10 mM maltose, and 5 mM BME at pH 8. Aliquots for monitoring time courses of digests were added to SDS−PAGE loading buffer and 1 mM EDTA to stop reactions. Factor X$_a$ digestions were performed at room temperature. SDS−PAGE was performed with 15% polyacrylamide gels.

RESULTS

Altered Binding Properties of BIR Arg Mutants. The functional role of the highly conserved BIR domain Arg was tested by comparing the binding of apoptosis stimulators to wild-type and mutant BIR2 regions of the baculovirus *O. pseudotsugata* Op-IAP and the *Drosophila* DIAP1. MBP (maltose binding protein)-BIR fusions were prebound to small (60−100 μL) amylose columns, to which MBP binds, and BIR−stimulator interactions were detected as BIR-dependent retention of stimulator proteins on the column. As seen in Figure 1, the MBP-BIR fusion containing the wild-type BIR2 region of Op-IAP (residues 95−199) bound a Hid-GST fusion (Hid residues 1−37 fused to glutathione *S*-transferase) and human Smac. Hid and Smac coeluted with MBP-BIR when the amylose column was washed with maltose (to elute MBP; lanes E$_1$ and E$_2$ in Figure 1). The two wash steps (lanes W$_1$ and W$_2$) following the stimulator load (lane L$_s$) were performed to ensure all excess stimulator had washed off the column before the final maltose elutions. The relative amounts of stimulator eluting during the load vs the first wash (W$_1$) varied a little from experiment to experiment due to small variations in column bed volume and the volumes of loaded stimulator. In control experiments, Hid and Smac did not bind to columns containing MBP alone (no BIR), and GST alone did not bind to the wild-type MBP-BIR2 (Figure 1C). This indicated that the observed stimulator binding was specific for the BIR region.

The MBP-BIR2 fusion of Op-IAP containing the highly conserved Arg mutated to Ala (Arg114Ala) was expressed and purified in the same manner as the wild-type fusion protein. In contrast to the wild-type protein, the mutant fusion did not bind to either Hid(1−37)-GST or Smac (Figure 1). Since the Arg to Ala mutation represents a drastic change in side chain character and size which could disrupt domain folding, the more conservative Arg114Lys mutation was generated and tested. However, as seen in Figure 1, the Arg114Lys mutant still showed greatly weakened binding to Smac and Hid, indicating that even the similar Lys could not functionally substitute for the highly conserved Arg in the Op-IAP BIR2 domain.

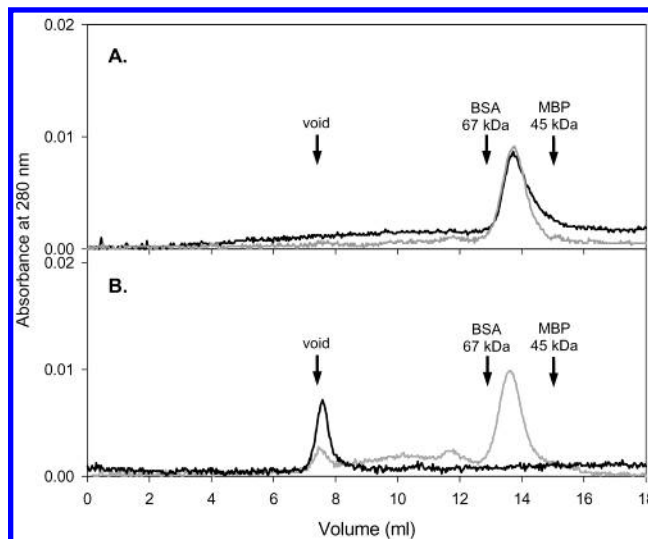Further analysis indicated that while the Ala and Lys mutant fusions were soluble and bound to amylose columns

FIGURE 2: Gel filtration of not refolded and refolded wild-type (A) and Arg114Lys mutant (B) MBP-Op-IAP-BIR2 fusion proteins on a Superdex 200 column. Traces for not refolded proteins are in black, and traces for refolded proteins are in gray. Arrows denote elution positions for bovine serum albumin (BSA), maltose binding protein (MBP), and high molecular weight dextran (void) used as molecular weight standards in separate runs. The fusions were loaded at 7 and 3 μM for the not refolded and refolded wild-type MBP-BIR2, respectively, and at 2 and 3 μM for the not refolded and refolded MBP-BIR2 Arg114Lys mutants, respectively. Peak identities were confirmed by SDS−PAGE analysis of collected column fractions.

during purification, they appeared to contain misfolded BIR domains. On a Superdex 200 gel filtration column the wild-type MBP-BIR2 fusion of Op-IAP (molecular mass 57 kDa) chromatographed as a single peak at a position between bovine serum albumin (67 kDa) and maltose binding protein cleaved from BIR (45 kDa), consistent with the wild-type fusion being monomeric (Figure 2). In contrast, the MBP-BIR2 Arg mutants of Op-IAP eluted primarily as a large aggregate at or just after the void volume of the column (the column exclusion limit is rated at 1.3 MDa by the manufacturer) (Figure 2). In addition, following cleavage of MBP from the BIRs with factor X$_a$, the wild-type BIR fragment remained soluble while the mutant BIRs immediately precipitated.

In an attempt to restore functional folds to the potentially misfolded mutant BIRs, the purified MBP-BIR fusions were denatured and refolded in vitro. Wild-type and mutant MBP-BIRs at concentrations ≤4 μM were denatured in 7 M urea and refolded by removal of urea by dialysis. The refolded wild-type MBP-BIR fusion of Op-IAP still chromatographed as a monomeric species in gel filtration (Figure 2) and retained its ability to bind Hid and Smac (Figure 3), demonstrating that BIR2 folding was reversible under these conditions. The refolding improved the aggregation state of the MBP-BIR Arg mutants as both the refolded Arg114Ala and the Arg114Lys fusions chromatographed predominately as single peaks coincident with the elution position of the wild-type fusion (Figure 2 for Arg114Lys). However, despite this improved behavior in gel filtration, the mutant fusions still showed little or no binding to Hid and Smac (Figure 3).

To assess if the function of other BIRs depends on the highly conserved Arg, we tested the effect of mutating the conserved Arg in the BIR2 of DIAP1. This BIR is required
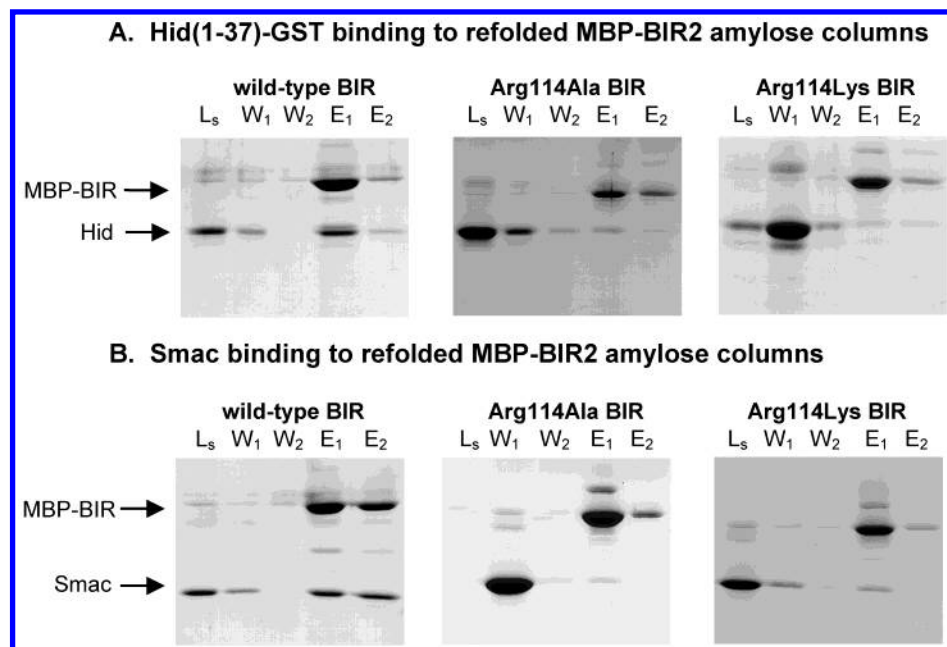
FIGURE 3: Binding of Hid(1−37)-GST (A) and Smac (B) to refolded MBP-Op-IAP-BIR2 fusions immobilized on amylose columns. The gel lanes show column elutions during application of Hid or Smac (L_s), washes with 1 mL of buffer each (W_1, W_2), and elution with 10 mM maltose (E_1, E_2). Hid and Smac were added at 4 μM with higher concentrations used for Hid binding to Arg114Lys and Smac binding to Arg114Ala.
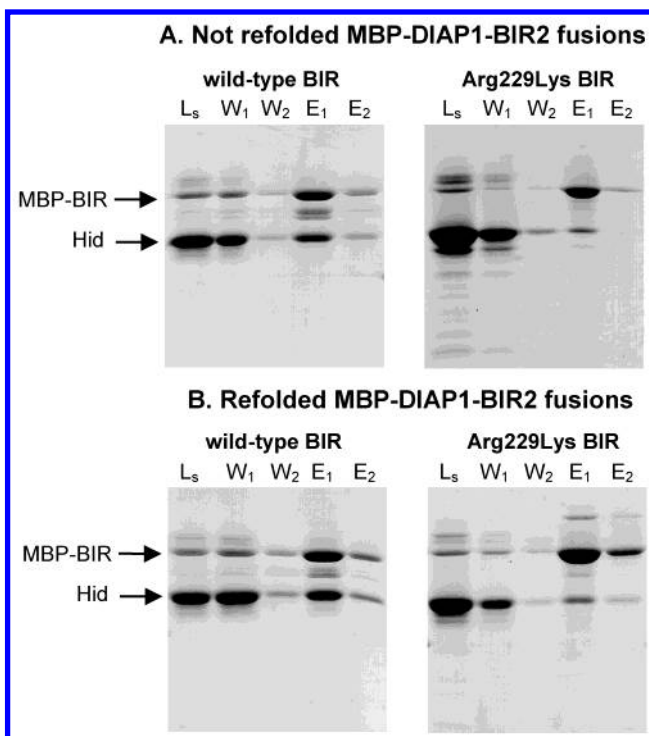

FIGURE 4: Binding of Hid(1−37)-GST to not refolded (A) and refolded (B) MBP fusions of wild-type and mutant DIAP1 BIR2 domains. The gel lanes show column elutions during application of 1 mL of 4 μM Hid (L_s), washes with 1 mL of buffer each (W_1, W_2), and elution with 10 mM maltose (E_1, E_2).

for the ability of DIAP1 to bind full-length Hid and N-terminal peptides of Hid and Grim (*8, 19*). MBP-BIR2 fusions were generated for residues 210−314 of DIAP1, corresponding to the same BIR2 region studied in Op-IAP. As seen in Figure 4A, the wild-type DIAP1 BIR2 fusion bound Hid(1−37)-GST, but binding was much weaker for the DIAP1 BIR2 fusion containing the conserved Arg (Arg229) mutated to Lys (Figure 4A).

As observed with the Op-IAP MBP-BIR mutants, gel filtration showed the DIAP1 Arg229Lys MBP-BIR2 mutant to be mostly aggregated and eluting as a sharp peak at or very near the void volume. Both the wild-type and Arg229Lys mutant DIAP1 fusions were denatured and refolded in vitro. Following refolding the wild-type MBP-BIR2 remained monomeric in gel filtration while the Arg229Lys mutant exhibited little or no protein eluting at the void volume. As with the Op-IAP fusion, the refolded wild-type MBP-BIR2 of DIAP1 retained binding to Hid (Figure 4B). However, the refolded mutant was still much weaker than the wild type in binding Hid (Figure 4B). The Arg229Lys mutant was also much weaker than the wild-type BIR2 in binding Smac for both refolded and not folded MBP-BIR fusions (not shown). Thus, in the context of an individual BIR domain, the highly conserved Arg is critical for the ability of the BIR2s of Op-IAP and DIAP1 to bind Hid(1−37) and Smac.

Role of Conserved Arg in BIR Domain Folding. Mutation of the highly conserved Arg strongly affects Hid and Smac binding despite the Arg being located on the opposite side of the BIR domain from the pocket where the N-termini of Smac, Hid, and Grim are known to bind human XIAP and *Drosophila* DIAP1 BIR domains (*16, 17, 19*). This suggests that the Arg mutations could be causing long-range perturbations to the BIR domain structure. Unfortunately, once cleaved from MBP by factor X_a proteolysis, the mutant BIRs exhibited poor solubility and purification characteristics, even after refolding, which precluded extensive analysis of the isolated mutant BIR domains. To determine the conformational state of the mutant BIRs, the MBP-BIR fusions were then examined for alterations in BIR domain zinc binding and in BIR domain fragmentation by limited proteolysis.

BIR domains contain a single zinc atom coordinated by three Cys residues and one His residue. The zinc site forms the scaffold underlying the surface groove where the N-terminal residues of Smac bind the BIR3 of XIAP and the

Table 1: Zinc Stoichiometries of MBP-BIR Fusions Determined by Atomic Absorption Spectroscopy

BIR2 domain fused to MBP	+zinc[a,c]	+EDTA[b,c]
Op-IAP, not refolded	1.0 ± 0.1 (3)	0.8 ± 0.3 (6)
Op-IAP, refolded	1.0 (1)	1.2 (1)
Op-IAP Arg114Lys, refolded	1.2 ± 0.2 (4)	0.5 ± 0.05 (5)
DIAP1, not refolded	0.9 ± 0.1 (4)	1.0 ± 0.2 (2)
DIAP1, refolded	0.9 (1)	0.8 (1)
DIAP1 Arg229Lys, refolded	0.8 ± 0.1 (2)	0.1 ± 0.02 (2)
none (MBP alone)	0.06 ± 0.04 (4)	ND

[a] Proteins were in buffer containing 2 μM zinc. [b] Proteins were treated with 10 mM EDTA overnight followed by dialysis against 0.1 mM EDTA. [c] Ranges are standard deviations for the number of determinations given in parentheses. All multiple determinations include at least two independently prepared protein samples.

N-terminal residues of Hid and Grim bind the BIR2 of DIAP1 (*16*, *17*, *19*). Thus, zinc binding should be sensitive to alterations in the binding groove for the apoptosis stimulators. Zinc binding by wild-type and mutant MBP-BIR2 fusions was assayed by atomic absorption to determine if structural alterations caused by mutation of the conserved Arg could propagate through the BIR domain to the zinc site and, hence, to the groove where N-termini of apoptosis stimulators bind. In the presence of buffers containing 2 μM ZnCl$_2$, wild-type Op-IAP and DIAP1 MBP-BIR fusions exhibited stoichiometric binding of zinc whether the proteins were refolded or not (average stoichiometries 0.9−1.0; Table 1). Zinc binding to MBP alone was minimal (stoichiometry 0.06; Table 1). Refolded Arg to Lys mutants exhibited average zinc stoichiometries of 0.8−1.2, indicating that they retained significant zinc binding (Table 1). Thus, the Arg mutants remained largely competent to bind zinc.

To test for differences in zinc affinity between wild-type and mutant proteins, the MBP-BIR fusions were treated with 10 mM metal chelator EDTA overnight followed by dialysis against buffer containing 0.1 mM EDTA. With this treatment the wild-type BIRs showed little or no loss of zinc binding whether or not the fusions had been refolded (Table 1). In contrast, mutation of the highly conserved Arg in the BIR2s of Op-IAP and DIAP1 increased the off-rate for zinc dissociation. The refolded Arg114Lys mutant of Op-IAP lost approximately 40% of its zinc while the refolded Arg229Lys mutant of DIAP1 lost approximately 90% of its zinc (Table 1). The greater zinc dissociation of the Arg mutants likely reflects a distorted conformation and/or increased flexibility of the polypeptide chain forming the zinc-binding site. When the Op-IAP Arg114Lys MBP-BIR was not refolded, its zinc stoichiometry dropped to an even lower 0.2 after EDTA treatment, consistent with it not being optimally folded during bacterial expression.

To further assess alterations in the structure of the mutant BIR domains, the susceptibility of wild-type and mutant MBP-BIR fusions to limited proteolysis was compared. Figure 5 shows fragmentation patterns for thermolysin digestions of wild-type and mutant MBP-Op-IAP-BIR2 and wild-type and mutant MBP-DIAP1-BIR2 fusions. Thermolysin preferentially cleaves N-terminal to Ile and Leu. Thermolysin digestion of the refolded or not refolded wild-type fusions generated two major fragments that corresponded closely in size to MBP and BIR2 fragments generated by digestion with factor X$_a$, which cleaves at a four-residue recognition site between MBP and the BIR2

domain (Figure 5A). The smaller thermolysin-generated fragment must contain the BIR2 since thermolysin digestion of MBP alone (refolded or not refolded) produced no discernible fragments (Figure 5B). The slightly larger size of the thermolysin-generated BIR fragment compared with the factor X$_a$-generated BIR fragment likely reflects cleavage at an Ile or Leu found in the linker between the MBP and BIR2 regions of the fusion protein or at the C-terminus of MBP.

In contrast to the wild-type fusion protein, thermolysin digestion of the Arg114Lys mutant of Op-IAP MBP-BIR fusion produced multiple small fragments along with a band corresponding to MBP (Figure 5). While the largest of the small fragments matches the size of the thermolysin-generated wild-type BIR2 fragment, smaller fragments are indicative of cleavage within the BIR2 domain. The BIR2 domain of Op-IAP does not contain any Ile but does contain six Leu residues, including one immediately after the conserved Arg. At least some of these Leu residues are more readily cleaved by thermolysin in the Arg114Lys mutant than in the wild-type BIR2. Enhanced fragmentation of the mutant BIR was also observed with the not refolded fusion proteins (Figure 5C). Thermolysin digestions of wild-type and Arg229Lys mutant MBP-BIR2 fusions of DIAP1 were similar to those of MBP-BIR fusions of Op-IAP. Digestion of DIAP1 wild-type MBP-BIR2 generated apparently full-length BIR while digestion of the Arg229Lys BIR mutant produced multiple small fragments (Figure 5D). The enhanced sensitivity to proteolysis of Arg mutants of Op-IAP and DIAP1 BIR2 domains suggests a generalized domain destabilization compared with the wild-type domains.

We were able to generate enough of the isolated DIAP1 BIR2 domain containing the Arg229Lys to analyze by circular dichroism (CD) spectroscopy. CD spectra were collected for the mutant DIAP1 BIR2 domain and for the wild-type BIR2 domains of Op-IAP and DIAP1 after cleavage and removal of MBP. As seen in Figure 6, both wild-type domains have similar spectra that exhibit strong negative peaks at 208 and 230 nm, indicative of secondary structure. While a negative peak at 208 nm is typical for α helix-containing proteins, the peak at 230 nm is more unusual and is often associated with Trp residues in distinct environments in folded proteins, including certain aromatic−aromatic interactions (*26*). The Arg229Lys mutant of DIAP1 loses this distinctive negative peak at 230 nm, but its CD spectrum still shows residual structure, including a minimum at approximately 210 nm instead the distinct peak at 200 nm typical of unfolded proteins (Figure 6). Analysis of the CD spectra using three different CD deconvolution programs implemented in CDPro (*27*) indicates that the helix content of the mutant drops by at least two-thirds (from 20% to 26% to 8%) while the mutant retains significant β sheet and turn structure (range of 19−60% for the three different programs). The retention of limited structure is consistent with the mutant's ability to still bind zinc (e.g., Table 1).

DISCUSSION

The highly conserved Arg residue of BIR domains is required for the functional folding of the isolated BIR2 domains of Op-IAP and DIAP1. While BIRs containing the conservative mutation of Arg to Lys showed some charac-
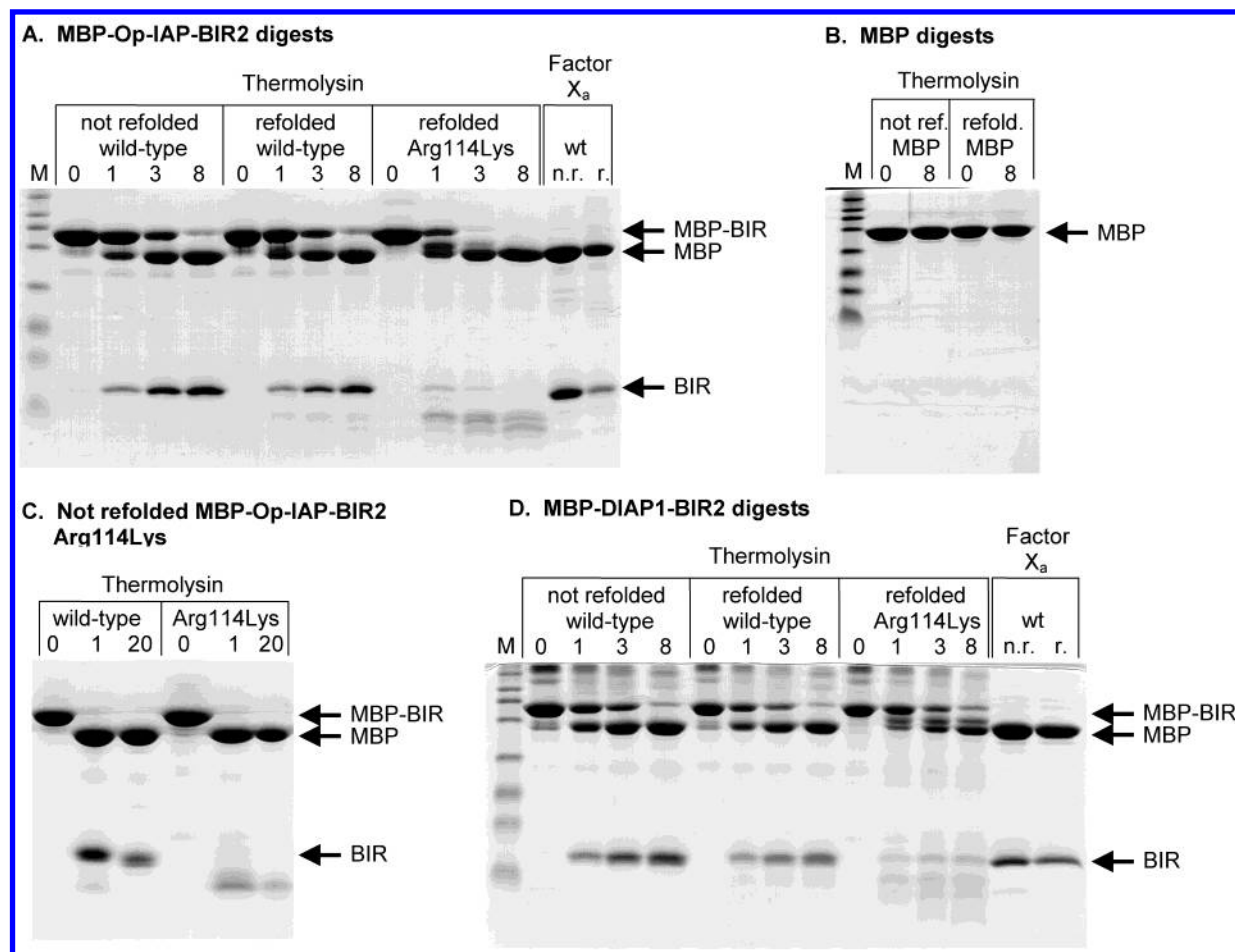
FIGURE 5: Time courses for protease digestions of Op-IAP and DIAP1 MBP-BIR2 fusions and of MBP. (A) Thermolysin digests of not refolded wild-type MBP-BIR (lanes 2−5), refolded wild-type MBP-BIR (lanes 6−9), and refolded Arg114Lys mutant MBP-BIR (lanes 10−13). Time points (0, 1, 3, 8) are in hours. Lanes 14 and 15 show factor X_a digests of not refolded (nr) and refolded (r) wild-type MBP-BIRs. (B) Thermolysin digests of not refolded (lanes 2 and 3) and refolded (lanes 4 and 5) MBP. Lanes 1 in (A) and (B) are molecular weight standards (175, 83, 62, 47.5, 32.5, 25, 16.5, and 6.5 kDa). (C) Thermolysin digests of not refolded wild-type and Arg114Lys MBP-Op-IAP-BIR2. (D) Same as (A) except with the corresponding DIAP1 MBP-BIR fusions. Digests in (A), (B), and (D) used 10 μM MBP-BIR or MBP and 1 μg/mL thermolysin at 4 °C. Digests in (C) used 42 μM MBP-BIR and 5 μg/mL thermolysin at room temperature.
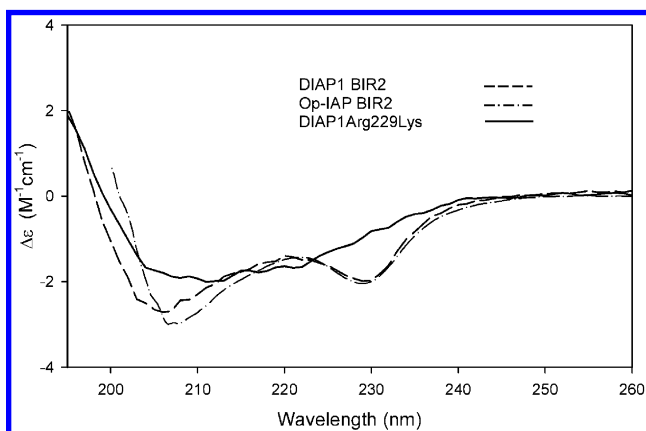

FIGURE 6: CD spectra of wild-type BIR2 domains of DIAP1 and Op-IAP and for the refolded Arg229Lys BIR2 domain of DIAP1. The wild-type and Arg229Lys BIR domains of DIAP1 were at 10 and 5 μM, respectively, and the Op-IAP BIR2 domain was at 25 μM.

teristics of wild-type domains, such as monomeric diffusion in gel filtration chromatography and stoichiometric binding of zinc, these mutant domains lost all ability to bind the apoptosis stimulators Hid and Smac. Hid and Smac require only 5−10 of their N-terminal residues to bind a surface groove on a side of the BIR domain opposite to that of the conserved Arg (*16*, *17*, *19*, *28*). Loss of Hid and Smac binding to the mutant BIR2s indicates that the effect of the Arg mutation propagates from one side of the BIR domain to the other. The Arg does lie in a helix that in the BIR3-Smac X-ray crystal structure is observed to bind to a more C-terminal region of Smac (*17*). However, this site appears to be of much lower importance since it cannot bind Smac molecules with a mutated N-terminal residue and since it exhibits suboptimal surface packing with Smac (*17*). Significant structural perturbation by Arg mutation was also evident in weakened zinc binding of mutant BIR domains. In wild-type BIR domains, the bound zinc is completely buried in a region between the Arg and the binding groove. The conserved Arg is not within the BIR polypeptide sequence that forms the zinc-binding site, and structures indicate that it does not directly contact any of the side chains forming the zinc-binding site. Structural perturbation in the Arg mutants was also evident in the enhanced fragmentation in proteolysis assays and the decreased α helix content and loss of a distinct 230 nm band in the DIAP1 Arg229Lys CD spectrum.

Examination of published BIR structures suggests several structural roles for the conserved Arg, of which a subset are specific to Arg and may be critical. NMR and X-ray crystal
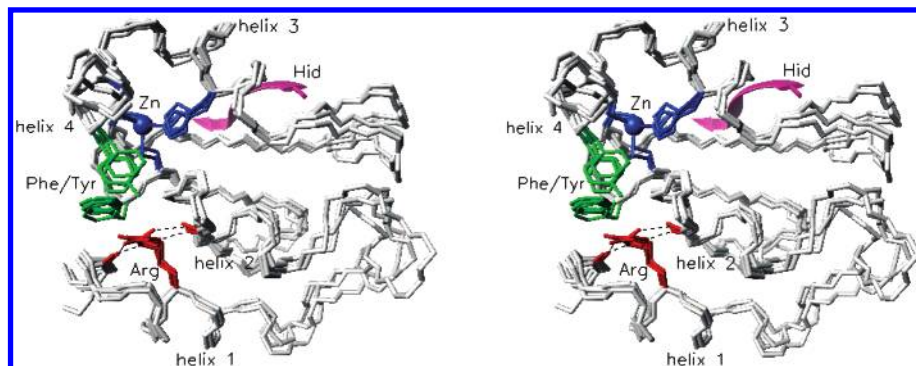
FIGURE 7: Overlay of BIR domain structures for survivin (*13*), XIAP [BIR2 (*18*) and BIR3 (*17*)], and DIAP1 [BIR2 (*19*)]. The structures are from PDB entries 1F3H, 1I3O, 1G73, and 1JD4, respectively. Backbone bonds are in light gray, the conserved Arg and proximal backbone oxygens are in red, the conserved aromatics are in green, and the residues coordinating zinc (sphere) are in blue. Representative Arg guanidino hydrogen bonds are displayed as dashed lines. The N-terminal five residues of Hid as bound to the DIAP1 BIR2 are shown as a pink ribbon to denote the location of the binding groove for the N-termini of Hid and Smac (from PDB entry 1JD6). The figure was rendered with the program MolMol (*32*).

structures of XIAP BIRs 2 and 3, cIAP1 BIR3, DIAP1 BIR2, and the single-BIR survivin show a BIR fold comprised of four α helices separated by a central three-strand β sheet (*10−15*, *18*, *19*). The highly conserved Arg sits near the N-terminus of the first helix which packs antiparallel to the second helix. In all structures, the Arg aliphatic side chain contributes to hydrophobic packing between the two helices while the positively charged guanidino group caps the C-terminus of the second helix, presumably stabilizing the helix dipole (Figure 7). The guanidino group is also consistently oriented to hydrogen bond to the backbone carbonyl oxygen (CO) of an Ala found near the end of the second helix, likely further anchoring the first two helices together (Figure 7). Distances between one guanidino NH atom and the CO are ≤3.1 Å in all of the X-ray crystal structures. In most structures the other guanidino NH can simultaneously donate a hydrogen bond to a CO preceding the first helix while the guanidino Nε can hydrogen bond to either of the two COs (Figure 7).

Crystal structures of BIR domains also show the Arg guanidino group packing against a pair of aromatic residues, one a Phe and the other Phe or Tyr, which are conserved in a majority of BIR sequences [residues 264 and 292 in DIAP1; the first aromatic is in 71% and the second in 94% of nonfragmented BIR sequences in the Pfam database (*24*)] (Figure 7). Positively charged side chains can form attractive cation−π interactions with aromatic groups, whose faces carry a partial negative charge from the π orbitals in the aromatic ring (*29−31*). These interactions are becoming recognized as important for protein folding and appear to occur with at least half the frequency of salt bridges (*31*). The two BIR aromatic residues are arranged edge to face, with the Arg guanidino group packed coplanar with the first Phe. Analysis with the program CaPTURE (*31*) detected significant (electrostatic energy ≤−1.0 kcal/mol and van der Waals energy ≤−1.0 kcal/mol) cation−π interactions between one of these aromatic groups and the Arg side chain in 11 of 12 BIR domain crystal structures in the Protein Data Bank (the 12 structures include each BIR chain in files 1E31 and 1F3H of survivin, 1I30 of XIAP BIR2, 1G73 of XIAP BIR3, and 1DJ4, 1DJ5, and 1DJ6 of DIAP1 BIR2 alone and complexed with different stimulator peptides). Since each of the aromatic groups lies one to two residues in sequence from a Cys zinc ligand, and the zinc site forms a scaffold

for the surface groove that binds the N-termini of Hid and Smac, structural alteration by Arg mutation could easily propagate to the Hid and Smac binding site. The two aromatic groups are 28 residues apart in sequence in these BIRs, and at least 33 residues from the conserved Arg, indicating that the cation−π interaction could be an important determinant for the tertiary fold of BIR domains.

The unique importance of Arg in the BIR domains may stem from its ability to form multiple hydrogen bonds and simultaneous cation−π interactions. While Lys should be able to contribute to the hydrophobic packing between the first two helices and to cap the end of the second helix, its single terminal amino group is too small to simultaneously donate hydrogen bonds to the CO in helix 2 and the CO preceding helix 1. In addition, the small size of the Lys terminal amino group compared with the Arg guanidinium likely makes Lys much less able to form simultaneous cation−π and hydrogen bond interactions (*31*). While it cannot be ruled out that mutation to Lys alters BIR folding by eliminating some van der Waals contacts made by the Arg guanidino group, such an effect would not seem to be a likely basis for Arg conservation. Changes in van der Waals interactions by amino acid variation can be compensated by amino acid variation elsewhere in proteins, as frequently observed in hydrophobic cores of homologous proteins.

While mutation of the conserved Arg appears to largely unfold the isolated BIR2 domains of Op-IAP and DIAP1, such drastic structural perturbation would likely be lessened in the context of the full-length IAPs where other regions of the IAP structure could partially stabilize the BIR2 folds. Nonetheless, the results from the isolated BIRs do reveal that the entire domain, including the surface groove that binds stimulators, is sensitive to alterations at the Arg position. In principle, this sensitivity provides a mechanism for allosteric regulation since binding of factors near the Arg site could thermodynamically couple through the BIR structure to the binding of apoptosis stimulators at the surface groove on the opposite side of the BIR domain. In this manner the second interface for Smac near the conserved Arg in the BIR3 of XIAP could stabilize the primary interaction with the Smac N-terminus. At the very least, the Arg appears to be critical for directing the BIR fold. While its hydrogen bonding and helix capping are likely important for local structure formation, such as orienting helix−helix packing,

the cation−π interaction is a greater determinant for global tertiary folding. The unique ability of Arg to participate in these multiple distinct types of interactions is the likely basis for its high conservation in the BIR domains.

ACKNOWLEDGMENT

REFERENCES

1. LaCasse, E. C., Baird, S., Korneluk, R. G., and MacKenzie, A. E. (1998) *Oncogene 17*, 3247−3259.
2. Nijhawan, D., Honarpour, N., and Wang, X. (2000) *Annu. Rev. Neurosci. 23*, 73−87.
3. Reed, J. C. (2001) *Trends Mol. Med. 7*, 314−319.
4. Deveraux, Q. L., and Reed, J. C. (1999) *Genes Dev. 13*, 239−252.
5. Holcik, M., and Korneluk, R. G. (2001) *Nat. Rev. Mol. Cell. Biol. 2*, 550−556.
6. Hay, B. A., Wassarman, D. A., and Rubin, G. M. (1995) *Cell 83*, 1253−1262.
7. Vucic, D., Kaiser, W. J., and Miller, L. K. (1998) *Mol. Cell. Biol. 18*, 3300−3309.
8. Vucic, D., Kaiser, W. J., and Miller, L. K. (1998) *J. Biol. Chem. 273*, 33915−33921.
9. McCarthy, J. V., and Dixit, V. M. (1998) *J. Biol. Chem. 273*, 24009−24015.
10. Hinds, M. G., Norton, R. S., Vaux, D. L., and Day, C. L. (1999) *Nat. Struct. Biol. 6*, 648−651.
11. Sun, C., Cai, M., Gunasekera, A. H., Meadows, R. P., Wang, H., Chen, J., Zhang, H., Wu, W., Xu, N., Ng, S. C., and Fesik, S. W. (1999) *Nature 401*, 818−822.
12. Sun, C., Cai, M., Meadows, R. P., Xu, N., Gunasekera, A. H., Herrmann, J., Wu, J. C., and Fesik, S. W. (2000) *J. Biol. Chem. 275*, 33777−33781.
13. Verdecia, M. A., Huang, H., Dutil, E., Kaiser, D. A., Hunter, T., and Noel, J. P. (2000) *Nat. Struct. Biol. 7*, 602−608.
14. Muchmore, S. W., Chen, J., Jakob, C., Zakula, D., Matayoshi, E. D., Wu, W., Zhang, H., Li, F., Ng, S. C., and Altieri, D. C. (2000) *Mol. Cell 6*, 173−182.
15. Chantalat, L., Skoufias, D. A., Kleman, J. P., Jung, B., Dideberg, O., and Margolis, R. L. (2000) *Mol. Cell 6*, 183−189.
16. Liu, Z., Sun, C., Olejniczak, E. T., Meadows, R. P., Betz, S. F., Oost, T., Herrmann, J., Wu, J. C., and Fesik, S. W. (2000) *Nature 408*, 1004−1008.
17. Wu, G., Chai, J., Suber, T. L., Wu, J. W., Du, C., Wang, X., and Shi, Y. (2000) *Nature 408*, 1008−1012.
18. Riedl, S. J., Renatus, M., Schwarzenbacher, R., Zhou, Q., Sun, C., Fesik, S. W., Liddington, R. C., and Salvesen, G. S. (2001) *Cell 104*, 791−800.
19. Wu, J., Cocina, A. E., Chai, J., Hay, B. A., and Shi, Y. (2001) *Mol. Cell 8*, 95−104.
20. Srinivasula, S. M., Datta, P., Kobayashi, M., Wu, J. W., Fujioka, M., Hegde, R., Zhang, Z., Mukattash, R., Fernandes-Alnemri, T., Shi, Y., Jaynes, J. B., and Alnemri, E. S. (2002) *Curr. Biol. 12*, 125−130.
21. Srinivasula, S. M., Hegde, R., Saleh, A., Datta, P., Shiozaki, E., Chai, J., Lee, R. A., Robbins, P. D., Fernandes-Alnemri, T., Shi, Y., and Alnemri, E. S. (2001) *Nature 410*, 112−116.
22. Chai, J., Shiozaki, E., Srinivasula, S. M., Wu, Q., Datta, P., Alnemri, E. S., Shi, Y., and Dataa, P. (2001) *Cell 104*, 769−780.
23. Huang, Y., Park, Y. C., Rich, R. L., Segal, D., Myszka, D. G., and Wu, H. (2001) *Cell 104*, 781−790.
24. Bateman, A., Birney, E., Durbin, R., Eddy, S. R., Howe, K. L., and Sonnhammer, E. L. (2000) *Nucleic Acids Res. 28*, 263−266.
25. Gobinda, S., and Sommer, S. S. (1990) *BioTechniques 4*, 404−407.
26. Woody, R. W., and Dunker, A. K. (1996) in *Circular dichroism and the conformational analysis of biomolecules* (Fasman, G. D., Ed.) pp 109−145, Plenum Press, New York.
27. Sreerama, N., Venyaminov, S. Y., and Woody, R. W. (2000) *Anal. Biochem 287*, 243−251.
28. Chai, J., Du, C., Wu, J., Kyin, S., Wang, X., and Shi, Y. (2000) *Nature 406*, 855−862.
29. Burley, S. K., and Petsko, G. A. (1986) *FEBS Lett. 203*, 139−143.
30. Dougherty, D. A. (1996) *Science 271*, 163−168.
31. Gallivan, J. P., and Dougherty, D. A. (1999) *Proc. Natl. Acad. Sci. U.S.A. 96*, 9459−9464.
32. Koradi, R., Billeter, M., and Wüthrich, K. (1996) *J. Mol. Graphics 14*, 51−55.